CellPress

Cancer Cell
Article

Merlin/*NF2* Loss-Driven Tumorigenesis Linked to CRL4^{DCAF1}-Mediated Inhibition of the Hippo Pathway Kinases Lats1 and 2 in the Nucleus

Wei Li,[1,*] Jonathan Cooper,[1,2] Lu Zhou,[3] Chenyi Yang,[4] Hediye Erdjument-Bromage,[5] David Zagzag,[6] Matija Snuderl,[6] Marc Ladanyi,[7] C. Oliver Hanemann,[3] Pengbo Zhou,[4] Matthias A. Karajannis,[8] and Filippo G. Giancotti[1,*]

[1]Cell Biology Program, Sloan Kettering Institute for Cancer Research, Memorial Sloan Kettering Cancer Center, New York, NY 10065, USA
[2]Sloan Kettering Division, Weill Graduate School of Medical Sciences, Cornell University, New York, NY 10065, USA
[3]Plymouth University Peninsula School of Medicine and Dentistry, Plymouth PL6 8BU, UK
[4]Department of Pathology and Laboratory Medicine, Weill Cornell Medical College, New York, NY 10065, USA
[5]Molecular Biology Program, Sloan Kettering Institute for Cancer Research, Memorial Sloan Kettering Cancer Center, New York, NY 10065, USA
[6]NYU Cancer Institute and Department of Pathology, NYU Langone Medical Center, New York, NY 10016, USA
[7]Department of Pathology and Human Oncology and Pathogenesis Program, Memorial Sloan Kettering Cancer Center, New York, NY 10065, USA
[8]NYU Cancer Institute and Department of Pediatrics, NYU Langone Medical Center, New York, NY 10016, USA
*Correspondence: liw@mskcc.org (W.L.), f-giancotti@ski.mskcc.org (F.G.G.)
http://dx.doi.org/10.1016/j.ccr.2014.05.001

SUMMARY

It is currently unclear whether Merlin/*NF2* suppresses tumorigenesis by activating upstream components of the Hippo pathway at the plasma membrane or by inhibiting the E3 ubiquitin ligase CRL4^{DCAF1} in the nucleus. We found that derepressed CRL4^{DCAF1} promotes YAP- and TEAD-dependent transcription by ubiquitylating and, thereby, inhibiting Lats1 and 2 in the nucleus. Genetic epistasis experiments and analysis of tumor-derived missense mutations indicate that this signaling connection sustains the oncogenicity of Merlin-deficient tumor cells. Analysis of clinical samples confirms that this pathway operates in *NF2*-mutant tumors. We conclude that derepressed CRL4^{DCAF1} promotes activation of YAP by inhibiting Lats1 and 2 in the nucleus.

INTRODUCTION

The tumor suppressor Merlin/*NF2* was identified in 1993 in patients affected by neurofibromatosis type 2 (NF2) and was later found to be mutated in sporadic meningiomas, ependymomas, and schwannomas; a large fraction of malignant pleural mesotheliomas; and a small percentage of other tumor types. Merlin is a multifunctional protein that shuttles between the cell cortex and the nucleus in a manner reminiscent of the cell adhesion and signaling component β-catenin. However, it remains unclear whether Merlin suppresses tumorigenesis by activating antimitogenic signals at the cell cortex or in the nucleus and by what molecular mechanism (Li et al., 2012 and references therein).

Studies in *Drosophila* suggest that Merlin combines with Expanded and Kibra at the cell cortex to activate the Hippo tumor suppressor pathway (Halder and Johnson, 2011). This pathway consists of a kinase cascade comprising the kinase Hippo (MST1/2 in mammals), the adaptor Salvador (Sav1), and the kinase Warts (Lats1/2). The final element, Warts/Lats, phosphorylates and inactivates the transcriptional coactivator Yorkie/YAP, suppressing Scalloped/TEAD-dependent transcription of genes involved in cell survival and proliferation (Hariharan and Bilder, 2006; Harvey and Tapon, 2007; Pan, 2010; Zhao et al., 2010a). In *Drosophila*, the Hippo pathway restrains cell proliferation and promotes apoptosis to limit organ size and to suppress the development of tumorous overgrowths (Hariharan and Bilder, 2006; Harvey and Tapon, 2007; Pan, 2010; Zhao et al.,

Significance

In spite of significant advances, the mechanism by which Merlin/*NF2* suppresses tumorigenesis has remained incompletely understood. We have found that Merlin translocates into the nucleus, where it inhibits the promitogenic E3 ubiquitin ligase CRL4^{DCAF1}. Here we provide evidence that CRL4^{DCAF1} promotes YAP-dependent transcription and oncogenesis by ubiquitylating and, thereby, inhibiting the Hippo pathway components Lats1 and 2. Analysis of clinical samples indicates that this signaling mechanism operates in *NF2*-mutant tumors. These results reveal the mechanism by which Merlin activates the Hippo pathway and suppresses tumorigenesis.

2010a). Genetic studies in mouse models and genomic analyses of human tumors indicate that Lats1/2 can function as a tumor suppressor and YAP as an oncogene, providing evidence that the function of the downstream segment of the Hippo pathway is evolutionarily conserved (Overholtzer et al., 2006; St John et al., 1999; Zender et al., 2006). Because mammalian Merlin can inhibit YAP- and TEAD-dependent transcription and deletion of *Yap* suppresses liver overgrowth and tumorigenesis in mice carrying a conditional ablation of *Nf2*, it has been proposed that Merlin suppresses tumorigenesis by activating the Hippo pathway (Zhang et al., 2010; Zhao et al., 2007). However, because YAP is necessary for the expansion of bipotential liver progenitors during development, this result does not necessarily imply that YAP signaling drives hepatocellular carcinoma development. In fact, analysis of The Cancer Genome Atlas and Cosmic data sets indicates that no Hippo pathway component is altered at a significant frequency in human liver cancer (Cerami et al., 2012). In addition, the upstream regulators of the Hippo pathway, and the way in which they are interconnected, have diverged after the separation of arthropods and chordates (Bossuyt et al., 2014), suggesting that Merlin inhibits Hippo signaling through divergent mechanisms in *Drosophila* and mammals.

We have found that the dephosphorylated, active conformer of mammalian Merlin suppresses tumorigenesis by inhibiting the E3 ubiquitin ligase CRL4^{DCAF1} in the nucleus (Li et al., 2010). Intriguingly, CRL4^{DCAF1} controls an oncogenic program of gene expression that includes TEAD target genes, suggesting that Merlin controls Hippo signaling by inhibiting CRL4^{DCAF1} (Li et al., 2010). Here we provide evidence that derepressed CRL4^{DCAF1} targets Lats1 and 2 for ubiquitylation and inhibition in the nucleus and, thus, activates YAP-driven transcription and oncogenesis.

RESULTS

Deregulated CRL4^{DCAF1} Induces Activation of YAP

To examine whether CRL4^{DCAF1} inactivates the Hippo signaling pathway, we examined *NF2*-mutant mesothelioma and schwannoma cells. Meso-33 mesothelioma cells undergo a complete proliferation arrest in response to re-expression of Merlin (Li et al., 2010) and do not possess genetic abnormalities at the *BAP1* locus, which is frequently mutated in malignant mesotheliomas devoid of *NF2* mutations (Bott et al., 2011). As anticipated, re-expression of Merlin induced robust phosphorylation of YAP at its major negative regulatory site, S127, which is phosphorylated by Lats1 and 2 in these cells (Figure 1A, lanes 1 and 2). Notably, expression of DCAF1 reduced phosphorylation of YAP at the same site, suggesting that CRL4^{DCAF1} can promote YAP signaling (Figure S1A available online).

We have shown previously that wild-type DCAF1 partially reverses the inhibition of proliferation induced by Merlin, whereas a mutant lacking the C-terminal Merlin-binding segment (DCAF1 1417X) completely reverses this process (Li et al., 2010). Intriguingly, although wild-type DCAF1 alleviated the ability of Merlin to induce phosphorylation of YAP, DCAF1 1417X suppressed it almost completely, suggesting that Merlin inactivates YAP by inhibiting CRL4^{DCAF1} (Figure 1A). In agreement with this hypothesis, depletion of DCAF1 induced phosphorylation of YAP and suppressed expression of the YAP target genes *CTGF* (Figure 1B; Figure S1B), *BIRC5*, and *CYR61* (Figure S1B). Moreover, it induced translocation of YAP/TAZ from the nucleus (Figures S1C and S1D) and suppressed transcription from a TEAD-dependent reporter (Figure S1E). These results indicate that CRL4^{DCAF1} is necessary for activation of YAP in *NF2*-mutant mesothelioma cells.

To extend these findings, we examined FC-1801 mouse schwannoma cells that were derived from *Nf2*$^{Flox/Flox}$ mice (Lallemand et al., 2009). In response to re-expression of Merlin, these cells undergo proliferation arrest and are no longer tumorigenic (Li et al., 2010). Expression of Merlin also induced phosphorylation of YAP in these cells (Figure S1F). Strikingly, although YAP/TAZ accumulated almost exclusively in the nuclei of these cells, even when they were confluent, silencing of DCAF1 provoked almost complete YAP/TAZ extrusion to the cytoplasm in most cells (Figure 1C; data not shown). Moreover, silencing of DCAF1 inhibited transcription from a TEAD-dependent reporter, although not as completely as overexpression of Merlin or dominant-negative TEAD (Figure 1D). Finally, in agreement with prior DNA microarray analyses (Li et al., 2010), overexpression of DCAF1 increased, and silencing of DCAF1 decreased, the expression of YAP target genes in FC-1801 cells (Figure S1G). Thus, derepression of CRL4^{DCAF1} activates YAP and induces TEAD-dependent transcription in *NF2*-mutant tumor cells.

CRL4^{DCAF1} Activates YAP without Inhibiting MST or Salvador

Unexpectedly, neither expression of Merlin nor silencing of DCAF1 increased phosphorylation of the activation loop of MST1 or MST2 (Figures S1H and S1I) (Deng et al., 2003; Glantschnig et al., 2002). In addition, neither of these manipulations promoted phosphorylation of Lats1 at the MST1/2 phosphorylation site T1079. Rather, these manipulations decreased this phosphorylation (Figures S1H and S1I), presumably by activating the negative feedback loops that restrain flux through the Hippo pathway (Genevet et al., 2010; Hamaratoglu et al., 2006; Xiao et al., 2011). These results suggest that the deregulation of YAP induced by loss of Merlin and activation of CRL4^{DCAF1} is not due to decreased activation of Lats1 by MST1/2.

To corroborate this hypothesis, we examined whether simultaneous depletion of MST1 and MST2 decreased phosphorylation of YAP in Merlin re-expressing or DCAF1-silenced Meso-33 cells. Notably, phosphorylation of YAP proceeded unabated upon both manipulations (Figures 1E and 1F). Moreover, this process was not affected by inactivation of the mammalian ortholog of Salvador, Sav1, an essential component of the core Hippo cassette (Lee et al., 2008; Tapon et al., 2002) (Figures 1G and 1H). Additional experiments revealed that silencing of Sav1 enhances TEAD-dependent transcription in Meso-33 cells, suggesting that the canonical Hippo pathway operates in these cells. However, expression of Merlin counteracted this process to a similar extent in control and Sav1-silenced cells (Figure S1J). As anticipated, silencing of DCAF1 and re-expression of Merlin failed to induce phosphorylation of YAP at S127 in cells depleted of Lats1 and 2 (Figures S1K and S1L). These findings indicate that the loss of Merlin and ensuing derepression of CRL4^{DCAF1} activate YAP independently of decreased flux through the core Hippo kinase cassette.

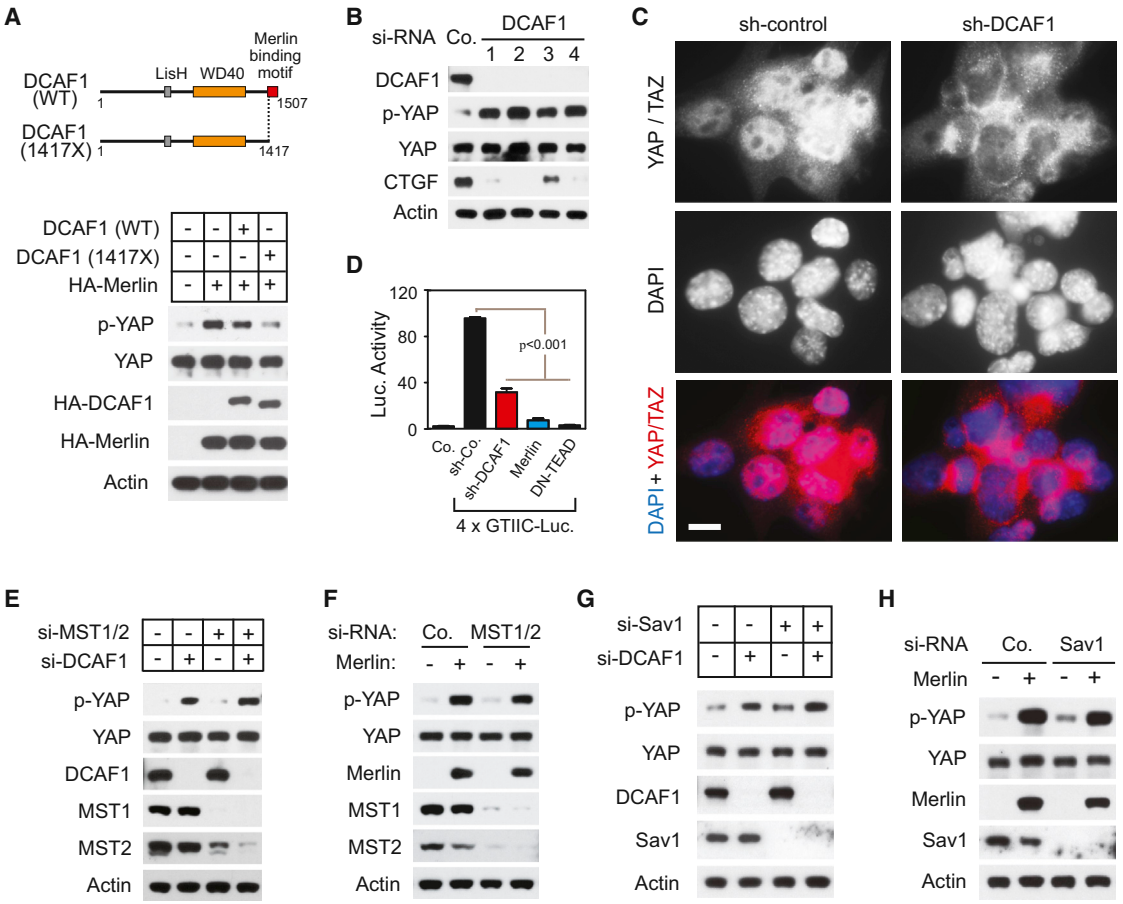

Figure 1. CRL4^{DCAF1} Controls YAP Activation and TEAD-Dependent Transcription in Merlin-Deficient Cells

(A) Schematics depicting wild-type (WT) and Merlin-resistant (1417X) DCAF1 (top). Meso-33 cells were transfected with HA-Merlin alone or in combination with HA-DCAF1 WT or 1417X and subjected to immunoblotting.

(B) Meso-33 cells were transfected with the indicated small interfering RNAs (siRNA) and examined by immunoblotting. Co, control.

(C) *Nf2* mutant FC-1801 cells were transduced with the indicated short hairpin RNAs (shRNAs) and subjected to immunofluorescent staining with anti-YAP/TAZ. Nuclei were stained with DAPI. Scale bar, 10 μm.

(D) FC-1801 cells were transduced with either a control shRNA, a shRNA targeting DCAF1, Merlin, or dominant-negative (DN) TEAD2 followed by a TEAD reporter and subjected to a luciferase (Luc.) assay. Error bars show ± SEM.

(E and G) Meso-33 cells were transfected with the indicated siRNAs and immunoblotted as indicated.

(F and H) Meso-33 cells were transfected with the indicated siRNAs and then with an empty vector or Merlin and immunoblotted as indicated.

See also Figure S1.

Lats1 and Lats2 Are Potential Substrates of CRL4^{DCAF1}

Motivated by the above findings, we examined the hypothesis that CRL4^{DCAF1} inhibits Lats1 and 2 by promoting their ubiquitylation. FLAG-hemagglutinin (HA)-DCAF1 associated efficiently with endogenous Lats1 and 2 but not with MST1 or 2 in human embryonic kidney 293T cells (HEK293T cells) (Figures 2A and 2B; Figure S2A). Mutagenesis indicated that the C-terminal segment of DCAF1 interacts directly with the kinase domain of Lats1 (Figures S2B and S2C). Because we could not produce recombinant Lats2 in bacteria, we were unable to verify that the C-terminal segment of DCAF1 also interacts directly with the kinase domain of Lats2. However, the homology between the kinase domains of Lats1 and 2 suggests that this is the case. Because the C-terminal fragment of DCAF1 contains the WD40 domain, which is involved in substrate recruitment (Angers et al., 2006; Jin et al., 2006), we hypothesized that CRL4^{DCAF1} recruits Lats1 and 2 to direct their ubiquitylation.

To examine whether Lats1 and 2 are ubiquitylated in vivo, HEK293T cells were transfected with His-ubiquitin and HA-tagged Lats1 or Lats2, treated with the proteasome inhibitor MG132, lysed in a guanidinium chloride-containing buffer, and subjected to pulldown with nickel beads. Anti-HA immunoblotting revealed that Lats1 is polyubiquitylated under these conditions (Figure 2C). Lower amounts of ubiquitylated Lats1 were recovered in the absence of MG132 (W.L and F.G.G., unpublished data), in consonance with the hypothesis that polyubiquitylation targets Lats1 for degradation through the proteasome. In contrast, Lats2 appeared to be oligoubiquitylated under the same experimental conditions (Figure 2D). Mass spectrometry indicated that Lats1 is modified by the addition of a single ubiquitin chain at K830 (Figure 2E; Table S1). K→R

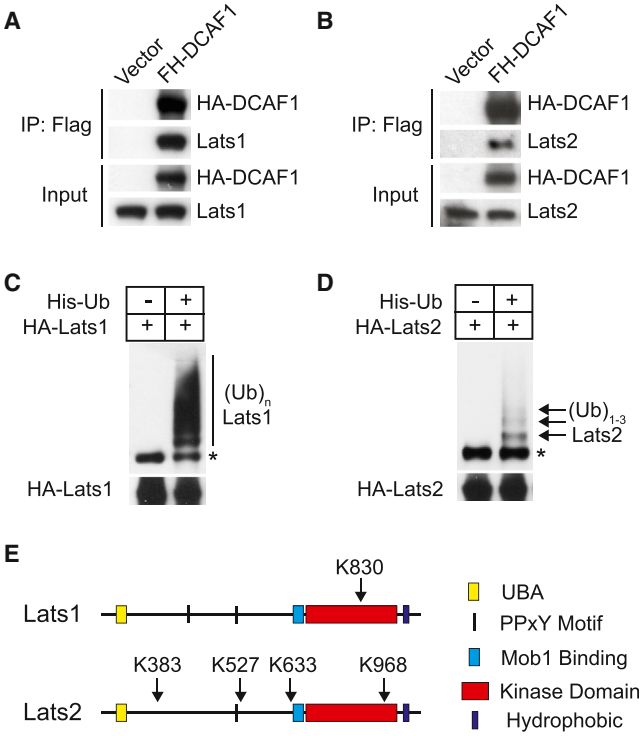

Figure 2. DCAF1 Interacts with Lats1/2, which Are Ubiquitylated In Vivo

(A and B) 293T cells transfected with an empty vector or FLAG-HA-tagged (FH) DCAF1 were immunoprecipitated (IP) with anti-FLAG and immunoblotted as indicated.

(C and D) Nickel precipitates and total lysates from 293T cells expressing HA-Lats1 or HA-Lats2 alone or in combination with His-ubiquitin (Ub) were immunoblotted with anti-HA. The asterisk points to a band that may correspond to Lats1/2 nonspecifically bound to nickel beads.

(E) Summary of ubiquitylation sites identified on Lats1/2 by mass spectrometry.

See also Figure S2 and Table S1.

substitution of residue 830 did not reduce polyubiquitylation of Lats1 (Figure S2D), pointing to compensatory ubiquitylation of additional lysine residues (King et al., 1996). In contrast, Lats2 was ubiquitylated at four sites (K383, K527, K633, and K968) (Figure 2E; Table S1). Simultaneous K→R substitutions at these residues did not reduce oligoubiquitylation of Lats2, again pointing to compensatory ubiquitylation of additional lysine residues (Figure S2E).

CRL4^{DCAF1} Promotes Proteasomal Degradation of Lats1

To examine whether CRL4^{DCAF1} promotes polyubiquitylation of Lats1, we performed in vivo ubiquitylation experiments. Expression of DCAF1 led to a large increase in polyubiquitylation of Lats1 in Meso-33 cells, and simultaneous expression of Merlin reversed this effect (Figure 3A). Moreover, although treatment with MG132 increased the level of polyubiquitylation of Lats1 in control HEK293T cells, it failed to produce this effect in DCAF1-depleted cells, indicating that CRL4^{DCAF1} is required for efficient polyubiquitylation of Lats1 (Figure S3A). To directly test whether CRL4^{DCAF1} mediates ubiquitylation of Lats1, we assembled recombinant CRL4^{DCAF1} in vitro and tested its ability

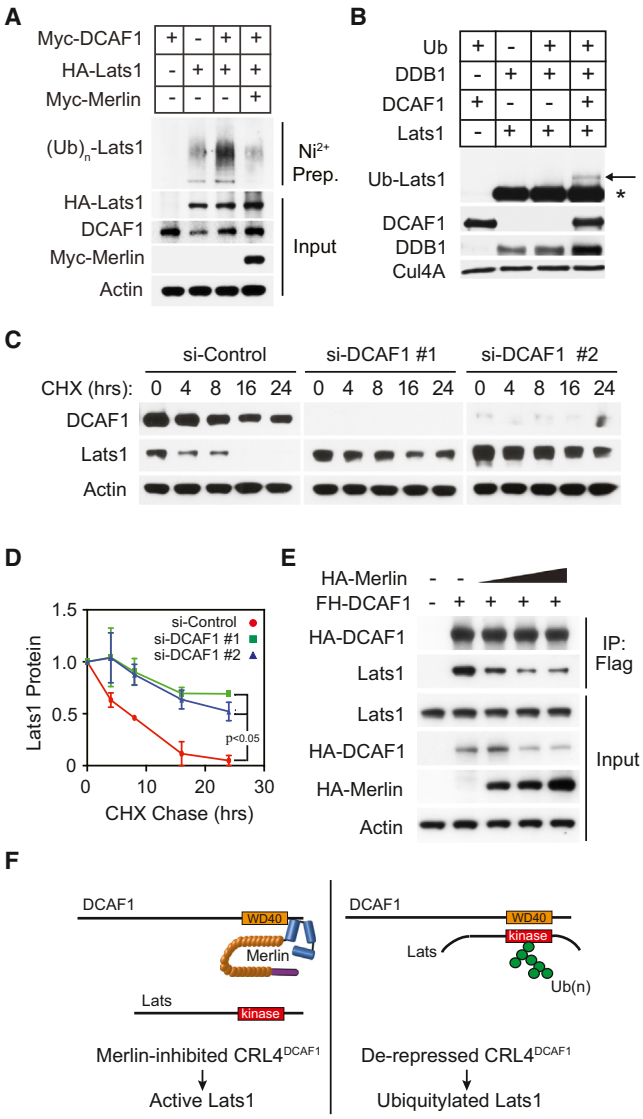

Figure 3. CRL4^{DCAF1} Ubiquitylates and Inhibits Lats

(A) Meso-33 cells were transfected with His-ubiquitin and the indicated recombinant proteins. Ubiquitylated proteins were nickel-purified (Ni^{2+} Prep.) and immunoblotted with anti-HA. Total lysates were immunoblotted as indicated.

(B) CRL4^{DCAF1} was reconstituted in vitro using purified recombinant Cul4A/Rbx1, DDB1, and DCAF1 and incubated with recombinant FH-Lats1 as indicated. Reaction mixtures were immunoblotted as indicated. The arrow points to a band that corresponds to ubiquitylated Lats1. The asterisk indicates a band that corresponds to purified Lats1.

(C) Meso-33 cells were transfected with the indicated siRNAs and subjected to a cycloheximide (CHX) chase assay. Lysates were immunoblotted as indicated.

(D) The results in (C) and an additional replicate experiment were quantified by densitometry. Error bars show ± SEM.

(E) 293T cells expressing FH-DCAF1 in combination with increasing quantities of HA-Merlin were immunoprecipitated with anti-FLAG and immunoblotted as indicated.

(F) Diagram illustrating a model based on the definition of the sequence requirements for binding of DCAF1 to Lats and of Merlin to DCAF1. The WD40 domain of DCAF1, which is implicated in substrate selection, binds directly to the kinase domain of Lats (right). Merlin binds through its FERM domain to the C-terminal segment of DCAF1, disrupting the association of DCAF1 with Lats (left).

See also Figure S3.

to ubiquitylate purified Lats1. We found that reconstituted CRL4 E3 ligase ubiquitylates Lats1 in vitro (Figure 3B). However, because we did not detect a robust extension of ubiquitin chains under the conditions of the assay, we infer that additional factors may be required for chain elongation in vivo.

It is well established that polyubiquitylation serves as a signal to target proteins for proteasome-mediated degradation. Because we had noticed that re-expression of Merlin and silencing of DCAF1 increase the steady-state levels of Lats1 in *NF2*-mutant cells (Figures S1H and S1I), we examined whether expression of DCAF1 causes the opposite effect. Stable expression of moderate levels of DCAF1 decreased the steady state levels of Lats1 in FC-1801 cells (Figure S3B). Furthermore, cycloheximide chase experiments demonstrated that silencing of DCAF1 prolongs the half-life of Lats1 in Meso-33 cells by more than 2-fold, indicating that CRL4^{DCAF1} promotes degradation of Lats1 (Figures 3C and 3D).

Because K830 lies within the kinase domain, polyubiquitylation of Lats1 may inhibit kinase activity by interfering with binding of ATP or recruitment of substrates. In addition, Lats1 and 2 contain an N-terminal ubiquitin-binding domain (UBA), which could bind in *cis* or in *trans* to one or more C-terminal ubiquitylated sequences, inducing conformational changes that interfere with kinase activity (Figure 2E). To examine whether polyubiquitylation inhibits the activity of Lats1, we expressed HA-Lats1 and His-ubiquitin in HEK293T cells and isolated total and His-ubiquitylated Lats1 by sequential affinity binding and elution (Figure S3C, top). An in vitro kinase assay indicated that ubiquitylated Lats1 possesses a severely diminished ability to phosphorylate glutathione S-transferase (GST)-YAP at S127 as compared to total Lats1 (Figure S3C, bottom). These results suggest that polyubiquitylation inhibits Lats1 by blocking its kinase activity and promoting its degradation.

CRL4^{DCAF1} Inhibits the Kinase Activity of Lats2

To investigate whether CRL4^{DCAF1} promotes ubiquitylation of Lats2, we performed in vivo ubiquitylation experiments. Ectopic expression of DCAF1 increased oligoubiquitylation of Lats2 to a large extent, and simultaneous expression of Merlin reversed this process (Figure S3D). Conversely, depletion of DCAF1 suppressed oligoubiquitylation of Lats2 (Figure S3E). In addition, we tested the ability of in vitro-assembled CRL4^{DCAF1} to promote ubiquitylation of recombinant Lats2. The results indicated that CRL4^{DCAF1} can ubiquitylate Lats2 in vitro (Figure S3F). Collectively, these results suggest that CRL4^{DCAF1} mediates oligoubiquitylation of Lats2.

In agreement with the model that mono- and oligoubiquitylation modify protein function without affecting protein stability (Chen and Sun, 2009), silencing of DCAF1 did not increase the steady-state levels of Lats2 (Figure S3G). Interestingly, Lats2 is ubiquitylated at K968 within the kinase domain, at K633 near the binding site for the coactivator Mob1/Mats, and at K527 near the PPXY motif involved in binding to YAP, suggesting that oligoubiquitylated Lats2 may exhibit a reduced ability to phosphorylate YAP/TAZ in vivo. To examine this hypothesis, we performed in-lysate kinase assays. Lysates from cells overexpressing HA-Lats2 were treated with the broad-specificity deubiquitylase USP8 or vehicle control and incubated with GST-YAP. Immunoblotting with anti-phosphorylated YAP (anti-p-YAP) revealed that deubiquitylated Lats2 possesses a greatly increased ability to phosphorylate GST-YAP at S127 compared with total Lats2 (Figure S3H, top). Immunoblotting confirmed that treatment with USP8 drastically diminishes the total levels of ubiquitylation of endogenous proteins (Figure S3H, bottom). Taken together, these findings indicate that ubiquitylation profoundly inhibits the kinase activity of Lats2.

Merlin Inhibits the Interaction between CRL4^{DCAF1} and Lats1

Prior studies have indicated that Merlin inhibits CRL4^{DCAF1} by binding through its 4.1 protein, Ezrin, Radixin, and Moesin (FERM) domain to the C-terminal segment of DCAF1. Intriguingly, patient-derived mutants of Merlin lacking the coiled-coil and C-terminal segments bind to DCAF1 but fail to suppress CRL4^{DCAF1}, suggesting that these latter segments are also required for the inhibition of ligase activity (Li et al., 2010). To test whether Merlin inhibits CRL4^{DCAF1} by interfering with substrate recruitment, we examined whether expression of Merlin interferes with the association of FLAG-HA-DCAF1 with endogenous Lats1 in HEK293T cells. Notably, cotransfection of increasing concentrations of HA-Merlin led to a dose-dependent reduction of the association of FLAG-HA-DCAF1 with Lats1 (Figure 3E). These results suggest that the coiled-coil and C-terminal segments of Merlin may occlude the binding site for Lats on the WD40 domain of DCAF1 (Figure 3F).

Nuclear Merlin Promotes Phosphorylation of YAP

Because CRL4^{DCAF1} accumulates predominantly in the nucleus (Li et al., 2010), we examined whether Merlin needs to enter this compartment to inactivate YAP and induce proliferation arrest. First we generated a fusion protein consisting of an N-terminal ERT2 domain joined by a short linker to full-length Merlin or, as a control, to dsRed (Figure S4A). The ERT2 domain drives passenger proteins to the nucleus in response to tamoxifen binding (Feil et al., 1997). As anticipated, treatment with tamoxifen induced accumulation of ERT2-Merlin and ERT2-DsRed in the nucleus (Figure S4B). Intriguingly, nuclear accumulation of Merlin, but not DsRed, induced phosphorylation of YAP and inhibited the proliferation of Meso-33 cells (Figures S4C and S4D). These results indicate that nuclear accumulation of Merlin is sufficient to induce phosphorylation of YAP and to inhibit proliferation.

To examine whether nuclear translocation of Merlin is required to induce proliferation arrest, we used mutational analysis. Analysis of a series of deletion mutants revealed a potential nuclear localization motif at position 24–27 (VRIV). Although alanine permutation of each residue or combinations of two or three residues within this motif partially inhibited nuclear accumulation of Merlin, a simultaneous alanine substitution of all four residues (24–27A) blocked this process completely (Figures 4A and 4B). A mutant form of Merlin lacking the VRIV sequence (Δ24–27) did not accumulate in the nucleus, even when Crm1-dependent nuclear export was blocked with leptomycin B, confirming that this motif acts as a noncanonical nuclear localization sequence (Figure 4C). Functional analysis revealed that re-expression of Merlin Δ24–27 or Merlin 24–27A does not induce phosphorylation of YAP or inhibit cell proliferation and soft agar growth in Meso-33 cells

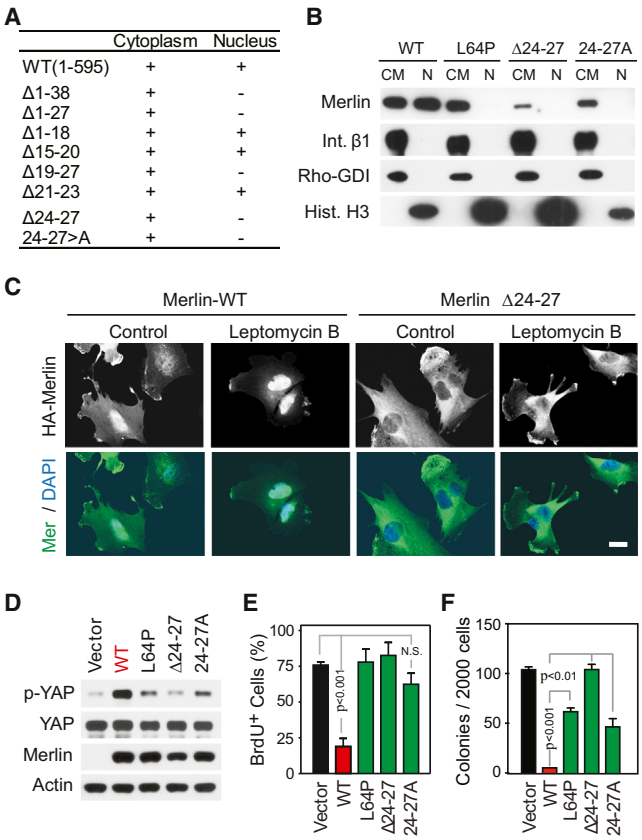

Figure 4. Nuclear Merlin Promotes YAP Phosphorylation and Inhibits Proliferation

(A) Summary of biochemical subcellular fractionation experiments. Cytoplasmic/membrane and soluble nuclear fractions from Meso-33 cells expressing Merlin or indicated mutants were immunoblotted for Merlin.

(B) Subcellular fractions from Meso-33 cells expressing wild-type Merlin or the indicated mutants were immunoblotted as indicated. CM, cytoplasmic/membrane fraction; N, nuclear fraction; Int. β1, integrin β1.

(C) Meso-33 cells expressing wild-type Merlin (Mer) or Merlin Δ24–27 were treated or not treated with leptomycin B to block nuclear export. Fixed cells were immunostained as indicated. Scale bar, 20 μm.

(D and E) Meso-33 cells expressing Merlin or its mutants were subjected to immunoblotting as indicated (D) or to a bromodeoxyuridine (BrdU) assay (E). N.S., not significant.

(F) FC-1801 cells transduced with wild-type Merlin or its mutants were subjected to a soft agar assay. Error bars show ± SEM.

See also Figure S4.

(Figures 4D–4F; Fig. S4E). These deficiencies do not arise from defective folding because these mutations are within the short and flexible N-terminal extension that distinguishes Merlin from Ezrin, Radixin, and Moesin proteins. Furthermore, both Merlin Δ24–27 and Merlin 24–27A associated efficiently with Angiomotin (Figure S4F), a recently identified Merlin-binding protein primarily localized at tight junctions (Yi et al., 2011). In fact, possibly resulting from their increased accumulation in the cytoplasm, these Merlin mutants combined with Angiomotin to a larger extent compared with wild-type Merlin (Figure S4F). These results indicate that Merlin needs to translocate into the nucleus to inactivate YAP and to suppress cell proliferation, suggesting that the two events are linked.

CRL4^{DCAF1} Inhibits Lats in the Nucleus

Based on immunofluorescence experiments on cells overexpressing tagged constructs or subcellular fractionation experiments excluding the nuclear fraction, it has been proposed that Lats1 and 2 execute their function at the cell cortex or in the cytosol (Toji et al., 2004; Yang et al., 2004; Yin et al., 2013). Because derepressed CRL4^{DCAF1} exerts its pro-oncogenic function in the nucleus (Li et al., 2010), we considered the possibility that its substrates Lats1 and 2 localize in this compartment. Subcellular fractionation experiments indicated that endogenous Lats1 and 2 accumulate in the nuclear fraction, whereas MST1 and Sav1 partition preferentially in the nonnuclear fraction in normal mesothelial Met-5A cells (Figure 5A). In fact, similar proportions of all of these signaling components were found in the nonnuclear and the nuclear fraction under sparse or confluent conditions (Figure 5A). Thus, although all of these components may shuttle in and out of the nucleus, MST1 and Sav1 are present predominantly in the nonnuclear fraction and Lats1 and 2 in the nuclear fraction at a steady state. Immunofluorescent staining with a rabbit monoclonal antibody against Lats1 confirmed that Lats1 accumulates in the nucleus in the large majority of Met-5A cells. Intriguingly, however, it also detected a fraction of the kinase at or near cell-to-cell junctions (Figure 5B). In agreement with the observation that Meso-33 cells do not express E-cadherin nor assemble adherens junctions, we did not detect endogenous Lats1 at cell junctions or at the cell cortex in these cells (Figure 5C), suggesting that deregulated CRL4^{DCAF1} does not target Lats1 at the cell cortex in *NF2*-mutant cells.

In the core Hippo kinase cassette, MST1 and 2 activate Lats1 by phosphorylating T1079. Activated Lats1 then undergoes autophosphorylation at S909 (Chan et al., 2005). Immunoblotting indicated that Lats1 becomes activated as YAP is phosphorylated and partially extruded from the nucleus in contact-inhibited Met-5A cells, confirming the specificity of these antibodies (Figures S5A and S5B). Notably, subcellular fractionation revealed that phosphorylated, active Lats1 accumulates almost exclusively in the nucleus in these cells (Figure 5D). Similar results were obtained with human liver epithelial HepG2 cells (Figure S5C) and primary mouse fetal liver progenitor cells (Figure S5D). These observations raise the possibility that MST or another upstream kinase moves into the nucleus to activate Lats. Irrespective of the mechanism involved, the predominant accumulation of CRL4^{DCAF1} and activated Lats in the nucleus is consistent with the hypothesis that CRL4^{DCAF1} binds to Lats and inhibits it in the nucleus.

Merlin Does Not Suppress Tumorigenesis from the Cell Cortex

Having noted that Lats1 partially localizes to the cell cortex in normal but not *NF2*-mutant cells (Figures 5B and 5C), we asked whether re-expression of Merlin modifies the subcellular localization of Lats1 in *NF2*-mutant cells. Upon transient transfection and ensuing overexpression, wild-type Merlin localized predominantly at lamellipodia and membrane ruffles in Meso-33 cells, presumably as a consequence of saturation of the nuclear import machinery, and it enhanced the recruitment of endogenous Lats1 to these locales (Figure S5E). Overexpression experiments indicated that HA-tagged Lats1 combines with

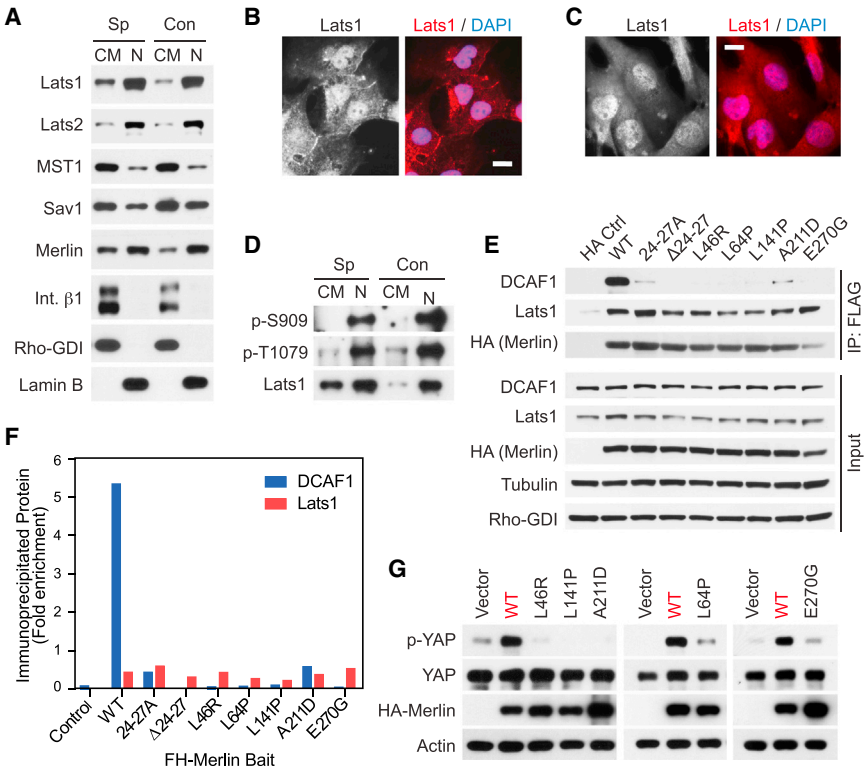

Figure 5. CRL4^{DCAF1} Inhibits Lats in the Nucleus

(A) Total lysates, cytosolic and crude membrane fractions (CM), and nuclear fractions (N) from sparse (Sp) or confluent (Con) Met-5A cells were immunoblotted as indicated.

(B and C) Sparse Met-5A cells and Meso-33 cells were stained with an anti-Lats1 antibody and DAPI. Scale bar, 20 μm.

(D) Endogenous Lats1 was immunoprecipitated with an anti-Lats1 antibody from cytosolic and crude membrane fractions and nuclear fractions from sparse or confluent Met5-A cells and immunoblotted as indicated.

(E) HEK293T cells were transfected with empty vector (HA Ctrl) or FLAG-HA-tagged Merlin (wild type or its mutants) and were lysed 24 hr later in RIPA buffer without SDS. FLAG immunoprecipitates were washed using RIPA buffer without SDS. FLAG immunoprecipitates and input were immunoblotted as indicated. Ctrl, control.

(F) Fold enrichment of immunoprecipitated DCAF1 and Lats1 was estimated by densitometry of blots in (E), where enrichment is expressed as the total density of the immunoprecipitated bands normalized to their respective inputs.

(G) Meso-33 cells expressing Merlin or its mutants were subjected to immunoblotting as indicated. See also Figure S5.

FLAG-HA-tagged Merlin in HEK293T cells (Figure S5F), in agreement with the recently proposed hypothesis that Merlin recruits Lats to the plasma membrane to promote its activation (Yin et al., 2013). Mutagenesis experiments indicated that the kinase domain of Lats1 interacts with the C-terminal coiled-coil segment of Merlin (Merlin 341–595) but not with its FERM domain (Merlin 341X) (Figures S5F and S5G). Together with the results of a recently published mutational analysis (Yin et al., 2013), these results suggest that Merlin can recruit Lats at the plasma membrane by binding through the N-terminal segment of its coiled-coil domain to the kinase domain of Lats.

To investigate the functional relevance of the interaction of Merlin with Lats1, we tested four patient-derived missense mutants that fail to accumulate in the nucleus (L46R, L64P, L141P, and A211D) and one that enters into the nucleus but does not bind to DCAF1 (E270G) (Li et al., 2010). In addition, we examined the two synthetic nuclear-defective mutants, Merlin 24–27A and Merlin Δ24–27 (Figures 4A–4C). Coimmunoprecipitation analysis indicated that recombinant wild-type Merlin combines with endogenous Lats1 much less efficiently than with CRL4^{DCAF1} in an extraction buffer containing 0.5% Triton X-100 but no ionic detergent (Figures 5E and 5F). In addition, although all nuclear-defective and patient-derived mutants of Merlin failed to associate with DCAF1 in this assay, none of them exhibited a reduced ability to interact with Lats1 (Figures 5E and 5F). Similar results were obtained by using radio-immunoprecipitation assay (RIPA) buffer containing 0.1% SDS (Figure S5H), although we note that this buffer may unfold the FERM domain of Merlin, exposing hydrophobic segments (Mani et al., 2011). In agreement with these results, none of the patient-derived mutants exhibited a reduced ability to recruit Lats1 to lamellipodia and membrane ruffles upon transient overexpression in Meso-33 cells (Figure S5E). In contrast, they all failed to induce phosphorylation of YAP at S127 (Figure 5G). These findings support the conclusion that Merlin suppresses tumorigenesis by inhibiting CRL4^{DCAF1} and, hence, stabilizing activated Lats in the nucleus rather than by recruiting Lats to the plasma membrane.

CRL4^{DCAF1} Promotes Tumorigenesis by Inhibiting Lats

To examine whether CRL4^{DCAF1} promotes oncogenesis by activating YAP, we conducted genetic epistasis experiments. As anticipated (Li et al., 2010), depletion of DCAF1 caused a profound proliferation arrest in Meso-33 cells (Figure 6A). Notably, expression of wild-type YAP and of YAP-5SA, which cannot be inactivated by Lats1/2 (Zhao et al., 2010b), rescued the DCAF1-silenced tumor cells from proliferation arrest in a manner proportional to their anticipated biological activity (Figure 6A). In addition, YAP-5SA enabled the DCAF1-silenced FC-1801 cells to grow in soft agar and to form tumors upon subcutaneous injection in nude mice (Figures 6B and 6C).

Next, we tested whether simultaneous depletion of Lats1 and 2 rescues the tumorigenic potential of DCAF1-silenced *NF2*-mutant cells. Simultaneous silencing of Lats1 and 2 largely reversed the proliferation arrest induced by depletion of DCAF1 in Meso-33 cells (Figure 6D). In support of the specificity of this effect, silencing of Lats1/2 did not enhance the ability of DCAF1-competent cells to proliferate in this assay (Figure 6D). Furthermore, silencing of Lats1/2 enabled DCAF1-depleted Meso-33 cells to grow in soft agar as efficiently as those expressing DCAF1

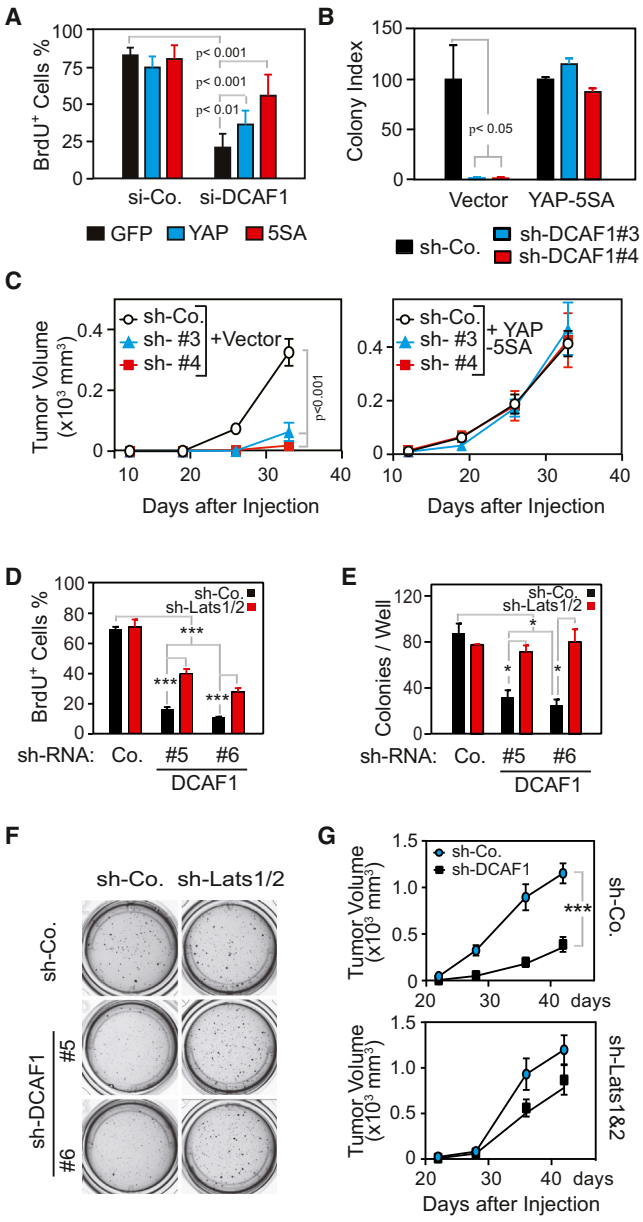

Figure 6. CRL4^{DCAF1}-Mediated Inhibition of Lats and Deregulated YAP Signaling Sustain the Oncogenic Properties of Merlin-Deficient Tumor Cells

(A) Meso-33 cells expressing GFP, YAP, or YAP-5SA were transfected with a SMARTpool control siRNA (si-Co.) or one targeting DCAF1 and subjected to a BrdU incorporation assay.

(B) FC-1801 cells expressing empty vector or YAP-5SA were transduced with the indicated shRNAs and subjected to a soft agar assay. The graph illustrates the results (± SEM) normalized to the relative control in the vector or YAP-5SA group.

(C) FC-1801 cells treated as in (B) were injected subcutaneously into nude mice.

(D) Meso-33 cells transduced with a control shRNA or shRNAs targeting Lats1/2 were transduced with a control shRNA or two different shRNAs targeting DCAF1 and subjected to a BrdU incorporation assay. ***$p < 0.001$.

(E) Meso-33 cells treated as in (D) were subjected to a soft agar assay. *$p < 0.001$.

(F) Typical cell colonies in individual culture wells in the 24-well plate are shown.

(G) FC-1801 cells transduced with a control shRNA (top) or shRNAs targeting Lats1/2 (bottom) were subsequently transduced with a control shRNA or a shRNA targeting DCAF1 and were injected subcutaneously into nude mice. Error bars show ± SEM. ***$p < 0.001$.

See also Figure S6.

(Figures 6E and 6F). Similar results were obtained with FC-1801 cells (Figure S6A).

Finally, we examined whether silencing of Lats1/2 rescues the tumorigenic ability of DCAF1-depleted FC-1801 cells. Intriguingly, silencing of Lats1/2 rescued the ability of DCAF1-depleted schwannoma cells to form tumors to a very large extent (Figure 6G; Figure S6B). We consider this effect specific because silencing of Lats1/2 alone did not increase tumor growth (Figures 6G; Figure S6B). Taken together, these findings indicate that derepression of CRL4^{DCAF1} promotes tumorigenesis of *NF2*-mutant cells by inactivating Lats1/2 and, hence, activating YAP.

CRL4^{DCAF1} Promotes YAP-Dependent Oncogenic Gene Expression in *NF2* Mutant Tumors

To explore the clinical relevance of the signaling mechanism we had identified, we first examined a panel of 11 human malignant mesothelioma cell lines carrying or not inactivating mutations at the *NF2* locus. Immunoblotting revealed that the *NF2*-mutant lines exhibited severely diminished levels of Lats1 but not Lats2 compared with *NF2* wild-type lines (Figure 7A; Figure S7A). In addition, all except one of the *NF2*-mutant cell lines displayed decreased phosphorylation of YAP, and four of seven lines displayed increased expression of the YAP target gene *CTGF* (Figure 7A; Figure S7A). These results are consistent with the conclusion that CRL4^{DCAF1} promotes the activation of YAP in mesothelioma, at least in part, by increasing degradation of Lats1.

To examine whether loss of *NF2* induces YAP-dependent oncogenic gene expression in clinical samples, we generated a gene expression signature reflective of CRL4^{DCAF1}-dependent YAP activity. Because only simultaneous depletion of YAP and TAZ induced Meso-33 cells to undergo a proliferation arrest as profound as that induced by depletion of DCAF1 (Figure 7B; Figure S7B), we used a DNA microarray analysis to compare the effect of inactivation of CRL4^{DCAF1} and simultaneous inactivation of YAP and TAZ on gene expression. Although depletion of YAP or TAZ did not lead to profound changes in gene expression in Meso-33 cells, simultaneous depletion of both coactivators caused a significant decline in gene expression, confirming that YAP and TAZ function redundantly to control gene expression in mesothelioma cells (Figure 7C). Notably, silencing of DCAF1 suppressed the expression of a large fraction of YAP/TAZ target genes (~39%) (Figures 7C and 7D; Figure S7C; Table S2). An ingenuity pathway analysis indicated that these genes comprise a large number of cell cycle genes controlled by the RB-E2F network (Figure S7D; Tables S3 and S4). In addition, silencing of DCAF1 enhanced the expression of a somewhat smaller fraction of the genes repressed by YAP/TAZ (~8%), including some transforming growth factor β target genes (Figures 7C and 7D; Figure S7D; Tables S3 and S5). These results indicate that CRL4^{DCAF1} controls a large fraction of the transcriptional output of YAP in *NF2*-mutant cells.

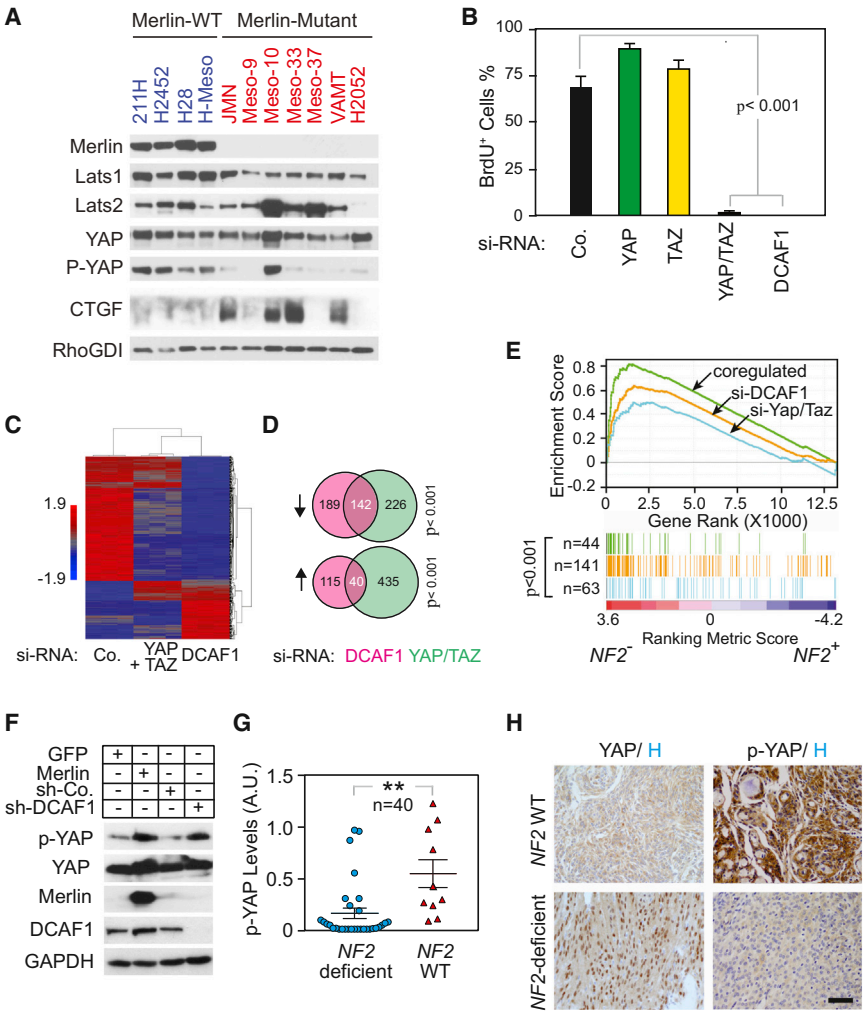

Figure 7. CRL4^{DCAF1} Controls YAP/TAZ-Dependent Gene Expression in NF2 Mutant Tumors

(A) A panel of human mesothelioma cell lines, including Merlin WT and Merlin mutant, were cultured under the same conditions. Lysates were immunoblotted as indicated.

(B) Meso-33 cells transfected with the indicated SMARTpool siRNAs were subjected to a BrdU incorporation assay.

(C) Meso-33 cells transfected with the indicated SMARTpool siRNAs were subjected to DNA microarray analysis and unsupervised hierarchical clustering.

(D) Venn diagram analysis of the genes downregulated or upregulated following depletion of DCAF1 or both YAP and TAZ. P values were obtained by Fisher's exact test.

(E) Genes whose expression depend on DCAF1 (orange), on both DCAF1 and YAP/TAZ (green), or on YAP/TAZ alone (blue) were subjected to GSEA in the gene expression profiles of human malignant mesothelioma classified by *NF2* mutation status (*NF2*-, mutant; *NF2*+, wild-type).

(F) Merlin-deficient primary human schwannoma cells were transduced with a vector encoding GFP, Merlin, and control or DCAF1 shRNAs and subjected to immunoblotting.

(G) Human meningioma and schwannoma samples classified by *NF2* mutation status were analyzed for YAP phosphorylation (A.U., arbitrary unit), which was normalized against total YAP expression. **$p < 0.01$.

(H) Representative formalin-fixed and paraffin-embedded *NF2* wild-type or *NF2*-deficient meningioma sections immunostained for YAP and phospho-YAP and counterstained with hematoxylin (H). Scale bar, 100 μm. Error bars show ± SEM.

See also Figure S7 and Tables S2 and S3–S6.

We next examined the gene expression profiles of 53 human mesotheliomas, 39 of which harbored a mutation or genomic loss at the *NF2* locus (Bott et al., 2011). Unsupervised hierarchical clustering strongly suggested that the *NF2*-mutant mesotheliomas were endowed with a largely distinct gene expression program (Figure S7E). Gene set enrichment analysis (GSEA) revealed that CRL4^{DCAF1}-activated genes were highly enriched in *NF2*-mutant mesotheliomas compared with the remaining mesotheliomas (Figure 7E). Intriguingly, among DCAF1-activated genes, those regulated via YAP and TAZ were enriched to an even higher extent, whereas those genes activated by Yap or TAZ alone were less enriched (Figure 7E). These results indicate that CRL4^{DCAF1} controls YAP/TAZ-dependent gene expression in *NF2*-mutant mesotheliomas.

To further examine the clinical relevance of our findings, we studied additional *NF2*-mutant tumor types. First, we analyzed primary human schwannoma cells freshly isolated from a patient affected by NF2. Prior studies had shown that re-expression of Merlin or silencing of DCAF1 suppresses the ability of these cells to proliferate in vitro (Li et al., 2010; Schulze et al., 2002). Interestingly, re-expression of Merlin and silencing of DCAF1 induced a similar level of phosphorylation of YAP in these cells (Figure 7F), suggesting that CRL4^{DCAF1} also controls the output of the Hippo pathway in freshly explanted, patient-derived *NF2* mutant schwannoma cells. We then examined activation of YAP in 40 human meningioma and vestibular schwannoma samples classified as *NF2*-mutant or not by using targeted genomic sequencing and immunoblotting with anti-Merlin (Figure S7F and Table S6). Immunoblotting tumor lysates with anti-p-YAP antibodies indicated that the level of phosphorylation of YAP was significantly lower in *NF2*-mutant tumors compared with that of other tumors (Figure 7G; Figure S7F). Finally, we examined the expression of YAP and phosphorylation of YAP on whole tissue sections of 31 meningiomas with a sufficient quality and quantity of formalin-fixed, paraffin-embedded tissue available. We observed strong nuclear staining of tumor cells for YAP in 16 of 22 samples (73%) and no staining in 6 of 22 samples (27%). In addition, we noted weak to absent cytoplasmic staining of tumor cells for P-YAP in 12 of 23 samples (52%) and moderate to strong staining in 11 of 23 samples (48%) (Figure 7H; Table S6). There was a strong positive correlation of nuclear YAP staining and weak or absent cytoplasmic p-YAP staining in tumors with low Merlin expression ($p = 0.001$ for YAP and $p = 0.001$ for phospho-YAP,

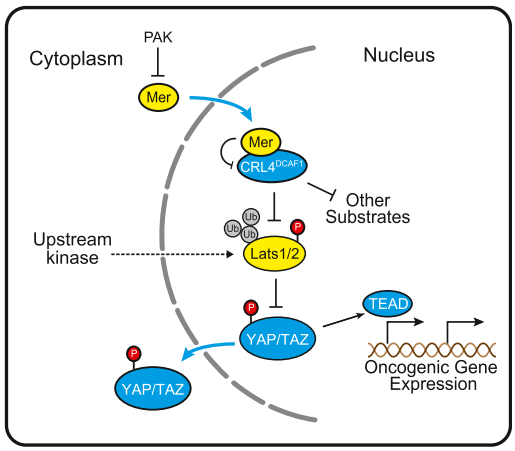

Figure 8. Model Illustrating the Mechanism by which CRL4^{DCAF1} Promotes Oncogenesis

In Merlin-deficient cells, CRL4^{DCAF1} promotes ubiquitylation of Lats1/2 and suppresses phosphorylation and inactivation of YAP. YAP promotes TEAD-dependent expression of proproliferative genes. It is likely that CRL4^{DCAF1} contributes to oncogenesis by ubiquitylating additional targets. In normal cells, antimitogenic signals promote the accumulation of the dephosphorylated, active form of Merlin. Upon translocation in the nucleus, this form of Merlin binds to DCAF1 and suppresses CRL4^{DCAF1} activity. This model does not exclude that Merlin activates the core Hippo kinase cascade by a distinct mechanism.

Mann-Whitney U test), indicating that loss of Merlin causes activation of YAP via reduced phosphorylation and increased accumulation in the nucleus. These clinical findings corroborate the hypothesis that CRL4^{DCAF1} inhibits Lats and, hence, activates YAP in *NF2*-mutant tumors.

DISCUSSION

Our results reveal that derepressed CRL4^{DCAF1} functions in the nucleus of *NF2*-mutant cells to promote activation of YAP. Mechanistically, CRL4^{DCAF1} binds directly to Lats1 and 2 and directs their conjugation to ubiquitin. Although Lats1 is polyubiquitylated and targeted for proteasome-dependent degradation, Lats2 is oligoubiquitylated at multiple sites, resulting in loss of kinase activity. As a consequence, active YAP and TAZ accumulate in the nucleus and function redundantly to support the oncogenic potential of *NF2*-mutant cells. These results indicate that derepressed CRL4^{DCAF1} promotes tumorigenesis by inhibiting Lats1 and 2 and, thus, promoting YAP/TAZ- and TEAD-dependent transcription (Figure 8).

Genetic epistasis experiments in *Drosophila* have suggested that Merlin cooperates with Expanded and Kibra to activate the core Hippo kinase cassette (Halder and Johnson, 2011). Although Merlin activates Hippo signaling and, thereby, also restricts activation of YAP in mammalian cells (Zhao et al., 2007), the molecular underpinnings of the connection of Merlin to the Hippo pathway have remained unclear. Recent studies have suggested that Merlin recruits Lats to the plasma membrane, facilitating its activation by an upstream kinase distinct from MST (Yin et al., 2013). Our results do not preclude the possibility that Merlin limits the proliferation of normal cells—for example, during contact inhibition—by multiple, possibly redundant, mechanisms, including those proposed above. However, they indicate that Merlin suppresses tumorigenesis largely, if not exclusively, by repressing CRL4^{DCAF1}-dependent ubiquitylation of Lats in the nucleus.

We observed that re-expression of Merlin induces phosphorylation and inactivation of YAP in *NF2*-mutant cells without increasing the levels of activation of MST1/2 or Lats1. In addition, Merlin-mediated inactivation of YAP proceeded unabated in the absence of Sav1, which functions as an essential adaptor linking MST1/2 to Lats1/2. These results suggest that Merlin does not restrict the activation of YAP by engaging the core kinase cassette but, rather, by regulating Lats1 and 2. These observations are consistent with prior evidence suggesting that Lats-mediated phosphorylation and inactivation of YAP can occur independently of MST1/2 in certain mammalian tissues (Yu et al., 2012; Zhou et al., 2009) and with a more recent study suggesting that Merlin facilitates Lats activation by an unidentified upstream kinase distinct from MST (Yin et al., 2013).

The results of our biochemical studies suggest that CRL4^{DCAF1} employs distinct mechanisms to inhibit Lats1 and 2. Upon DCAF1-mediated recruitment to the ligase complex, Lats1 is polyubiquitylated and, hence, targeted for proteasome-mediated degradation. In contrast, Lats2 is oligoubiquitylated at multiple sites, including at lysines in the kinase domain, near the Mob1-binding site, and near the PPXY motif required for interaction with YAP. Presumably as a result of these multiple modifications, Lats2 becomes inactive. Future studies will be required to determine the impact of each one of these modifications on the kinase activity of Lats2 and its interaction with substrates or necessary cofactors. Notably, both Lats1 and Lats2 possess an N-terminal UBA domain, suggesting the possibility that an intramolecular association of this domain with a C-terminal ubiquitylated sequence motif may contribute to maintain the two kinases in an inactive state in *NF2*-mutant tumor cells.

To examine the relevance of CRL4^{DCAF1}-mediated inhibition of Lats1/2 in *NF2* loss-driven oncogenesis, we reconstituted *NF2*-mutant cells with wild-type and mutant forms of Merlin. Deletion or alanine substitution of a short nuclear localization sequence prevented Merlin from interacting with CRL4^{DCAF1} and from suppressing the activation of YAP and cell proliferation. Conversely, tamoxifen-induced translocation of ERT2-Merlin in the nucleus and binding to CRL4^{DCAF1} resulted in the inhibition of YAP and cell proliferation. Furthermore, analysis of a large panel of patient-derived missense mutants of Merlin, which do not combine with CRL4^{DCAF1} as a result of their inability to enter into the nucleus and/or to bind to the Merlin-binding segment of DCAF1 (Li et al., 2010), revealed that all of them exhibit a severely reduced capacity to inhibit the activation of YAP and cell proliferation. Finally, in vitro and in vivo genetic epistasis experiments demonstrated that YAP and TAZ are necessary to maintain the oncogenicity of *NF2*-mutant tumor cells and that simultaneous inactivation of Lats1 and 2 rescues the oncogenicity of DCAF1-depleted *NF2*-mutant tumor cells. In our view, these results provide strong genetic evidence that Merlin suppresses tumorigenesis by inhibiting CRL4^{DCAF1} and, hence, increasing the levels of active Lats in the nucleus.

Based on the apparently prevalent localization of Hippo pathway components at the cell cortex or in the cytoplasm in *Drosophila*, it has been proposed that activated Lats phosphorylates YAP in the cytoplasm, preventing its accumulation in the nucleus through redundant mechanisms, such as binding to 14-3-3 or β-TRCP-mediated ubiquitylation (Dong et al., 2007; Zhao et al., 2007, 2010b). Consistently, overexpressed tagged forms of Lats1 and 2 accumulate predominantly in the cytosol or at centrosomes, respectively (Toji et al., 2004; Yang et al., 2004), whereas a mutant form of YAP that cannot be phosphorylated by Lats accumulates in the nucleus and promotes TEAD-dependent transcription and oncogenesis (Zhao et al., 2007). Because overexpression can saturate the nuclear import machinery and exogenous tags can interfere with transport into the nucleus of recombinant proteins, we examined the localization of endogenous Lats in mammalian cells by using immunofluorescence staining and subcellular fractionation. We found that endogenous Lats accumulates in the nucleus independently of growth conditions. Importantly, phosphorylated and activated Lats was almost exclusively found in the nucleus. These observations suggest that MST1/2 or another unidentified upstream kinase phosphorylates and activate Lats in the nucleus. Activated Lats, in turn, phosphorylates YAP, promoting its extrusion from the nucleus.

Our results do not exclude the possibility that Merlin may have additional functions at the cell cortex and, in fact, may also regulate the Hippo pathway from this location. Of note, we observed that Merlin can bind, albeit weakly, to Lats1 and Lats2, and we detected a fraction of Lats1 near the plasma membrane in normal mesothelial cells undergoing contact-mediated inhibition of proliferation. However, in contrast to the results of a more limited but similar analysis (Yin et al., 2013), we found that mutations that abolish the tumor suppressor function of Merlin do not interfere with its ability to bind to Lats1 and recruit it to the cell cortex. However, they consistently fail to bind to CRL4^{DCAF1} and to inactivate YAP. These results confirm that Merlin's function at the cell cortex is insufficient to suppress tumorigenesis.

We speculate that the signaling pathway we have delineated may have evolved after the separation of chordates from arthropods to provide additional control over the function of YAP. In fact, *Drosophila* Merlin contains a glycine residue at the position corresponding to E270 in human Merlin, a substitution that is predicted to abolish interaction with DCAF1 (Li et al., 2010). Moreover, the *Drosophila* ortholog of DCAF1, Mahjong (Tamori et al., 2010), does not contain a C-terminal Merlin-binding segment. These considerations suggest that the interaction of Merlin with CRL4^{DCAF1} has evolved in chordates to function as a clamp to restrain activation of YAP. In this model, Merlin and CRL4^{DCAF1} act as a negative and a positive component of a switch that fine-tunes the activation of YAP in mammalian cells. Inactivation of *NF2* eliminates the clamp, causing deregulated YAP/TEAD-dependent transcription of prosurvival and mitogenic genes. It remains to be examined whether this clamp on the activation of YAP also operates during development to limit stem cell self-renewal, organ size, and cell fate specification, as is anticipated from the known physiological function of YAP and its deregulation following inactivation of *NF2* during tumorigenesis.

We validated the relevance of our findings for human tumorigenesis by using a variety of approaches. First, genetic manipulation indicated that re-expression of Merlin and silencing of DCAF1 inhibit activation of YAP and cell proliferation in primary schwannoma cells from NF2 patients. Second, immunoblotting and immunostaining of meningioma and vestibular schwannoma samples revealed a striking correlation between the loss of Merlin and the activation of YAP. Third, analysis of a panel of human mesothelioma lines indicated that deletion of *NF2* correlates with reduced levels of Lats1 protein and increased activation of YAP. Finally, GSEA demonstrated that the gene expression program regulated by CRL4^{DCAF1} through activation of YAP/TAZ is highly enriched in *NF2*-mutant mesotheliomas compared with those lacking *NF2* alterations.

We note that simultaneous depletion of Lats1 and 2 did not completely rescue the ability of DCAF1-silenced *NF2*-mutant cells to overproliferate in vitro and in vivo, suggesting that CRL4^{DCAF1} may have additional substrates that contribute to its pro-oncogenic function. RORα, which has been identified recently as a CRL4^{DCAF1} substrate and exhibits severely reduced expression in human breast cancers (Lee et al., 2012), is a potential candidate, but other, still unidentified substrates may contribute as well. These considerations suggest that entry of Merlin into the nucleus and inhibition of CRL4^{DCAF1} may have evolved to limit not only the activation of YAP but also that of additional pro-oncogenic signals. In addition to their biological implications, these findings indicate that pharmacological targeting of CRL4^{DCAF1} is a rational approach for the treatment of neurofibromatosis type 2 and malignant pleural mesothelioma. We suggest that, because CRL4^{DCAF1} may promote oncogenesis through multiple mechanisms, CRL4^{DCAF1} inhibitors may display enhanced efficacy in *NF2*-mutant tumors compared with drugs that interfere with the interaction of YAP with TEAD (Jiao et al., 2014; Liu-Chittenden et al., 2012).

EXPERIMENTAL PROCEDURES

Patients and Tumor Samples

Human studies were approved by the institutional review boards of MSKCC, NYU-Langone Medical Center, and the Plymouth University Peninsula School of Medicine and Dentistry (see details in Supplemental Experimental Procedures).

Subcellular Fractionation

Nuclear and non-nuclear fractions were prepared using NE-PER nuclear and cytoplasmic extraction reagents following the manufacturer's instructions (Thermo Fisher Scientific).

Immunofluorescent Staining

Cells were fixed with 4% paraformaldehyde for 20 min and permeabilized with 0.3% sodium deoxycholate and 0.3% Triton X-100 for 30 min on ice. After blocking with 5% BSA, samples were incubated overnight at 4°C with primary antibodies diluted in PBS/2.5% BSA/0.05% Triton X-100. After washing with PBS/0.1% Triton X-100, samples were incubated with secondary antibodies diluted as described above for 2 hr at 4°C. Samples were finally washed with PBS/0.1% Triton X-100, rinsed with PBS, and mounted in Gelvatol.

In Vitro Ubiquitylation Assay

Affinity-purified recombinant proteins, including E1 (Calbiochem), E2 (UBCH5c), GST-Cul4A, His-Rbx1, GST-DDB1, His-ubiquitin, and FLAG-hemagglutinin (FH)-DCAF1 and FH-Lats1 (purified from HEK293T cells) were incubated in 20 μl reaction buffer (50 mM Tris-HCl [pH 7.5], 0.2 M NaCl, 10 mM

$MgCl_2$, 4 mM ATP, and 1 mM dithiothreitol) at 25°C for 2 hr. Reactions were terminated by boiling in SDS loading buffer.

Soft Agar and Tumorigenicity Assay

For the soft agar assay, cells were trypsinized, resuspended in complete medium, and plated in 0.34% low melting temperature agarose (FMC Bioproducts) in complete medium at 2 $\times 10^4$ (Meso-33 cells) or 1.2 $\times$ 10^4 (FC-1801 cells) per well in 24-well Ultra Low cluster plates (Costar). For the tumorigenicity assay, 1 $\times$ 10^6 FC-1801 cells were suspended in Ca/Mg-free PBS and injected subcutaneously into the right flank of nude mice. Tumor volumes were determined by caliper measurement. Animal studies were conducted in accordance with protocols approved by the Institutional Animal Care and Use Committee of MSKCC.

Statistical Methods

Statistical significance was determined by Student's t test unless indicated otherwise.

ACCESSION NUMBER

Microarray data are available in the Gene Expression Omnibus under accession number GSE56157.

SUPPLEMENTAL INFORMATION

Supplemental Information includes Supplemental Experimental Procedures, seven figures, and six tables and can be found with this article online at http://dx.doi.org/10.1016/j.ccr.2014.05.001.

ACKNOWLEDGMENTS

We thank I. Farrance, M. Giovannini, K. Guan, S. Jhanwar, D. Lim, M. Pagano, and D. Pan for reagents, R. Mukherjee and N. Antao for experimental assistance, the core facilities of MSKCC and NYU-Langone Medical Center for sample processing and analysis, and members of the F.G.G. laboratory for discussions. This work was supported by CTF Young Investigator Award 2009-01-013 (to W.L.) and NIH grants R01 CA152975 (to F.G.G.), S10 OD010591 (to the Microchemistry and Proteomics Core Laboratory of MSKCC), UL1 TR000038 (to the BioRepository and Immunohistochemistry Core Laboratory of NYU-Langone Medical Center), and P30 CA08748 (to MSKCC).

Received: July 1, 2013
Revised: February 14, 2014
Accepted: May 1, 2014
Published: July 14, 2014

REFERENCES

Angers, S., Li, T., Yi, X., MacCoss, M.J., Moon, R.T., and Zheng, N. (2006). Molecular architecture and assembly of the DDB1-CUL4A ubiquitin ligase machinery. Nature *443*, 590–593.

Bossuyt, W., Chen, C.L., Chen, Q., Sudol, M., McNeill, H., Pan, D., Kopp, A., and Halder, G. (2014). An evolutionary shift in the regulation of the Hippo pathway between mice and flies. Oncogene *33*, 1218–1228.

Bott, M., Brevet, M., Taylor, B.S., Shimizu, S., Ito, T., Wang, L., Creaney, J., Lake, R.A., Zakowski, M.F., Reva, B., et al. (2011). The nuclear deubiquitinase BAP1 is commonly inactivated by somatic mutations and 3p21.1 losses in malignant pleural mesothelioma. Nat. Genet. *43*, 668–672.

Cerami, E., Gao, J., Dogrusoz, U., Gross, B.E., Sumer, S.O., Aksoy, B.A., Jacobsen, A., Byrne, C.J., Heuer, M.L., Larsson, E., et al. (2012). The cBiol.cancer genomics portal: an open platform for exploring multidimensional cancer genomics data. Cancer Discov. *2*, 401–404.

Chan, E.H., Nousiainen, M., Chalamalasetty, R.B., Schäfer, A., Nigg, E.A., and Silljé, H.H. (2005). The Ste20-like kinase Mst2 activates the human large tumor suppressor kinase Lats1. Oncogene *24*, 2076–2086.

Chen, Z.J.J., and Sun, L.J.J. (2009). Nonproteolytic functions of ubiquitin in cell signaling. Mol. Cell *33*, 275–286.

Deng, Y., Pang, A., and Wang, J.H. (2003). Regulation of mammalian STE20-like kinase 2 (MST2) by protein phosphorylation/dephosphorylation and proteolysis. J. Biol. Chem. *278*, 11760–11767.

Dong, J., Feldmann, G., Huang, J., Wu, S., Zhang, N., Comerford, S.A., Gayyed, M.F., Anders, R.A., Maitra, A., and Pan, D. (2007). Elucidation of a universal size-control mechanism in *Drosophila* and mammals. Cell *130*, 1120–1133.

Feil, R., Wagner, J., Metzger, D., and Chambon, P. (1997). Regulation of Cre recombinase activity by mutated estrogen receptor ligand-binding domains. Biochem. Biophys. Res. Commun. *237*, 752–757.

Genevet, A., Wehr, M.C., Brain, R., Thompson, B.J., and Tapon, N. (2010). Kibra is a regulator of the Salvador/Warts/Hippo signaling network. Dev. Cell *18*, 300–308.

Glantschnig, H., Rodan, G.A., and Reszka, A.A. (2002). Mapping of MST1 kinase sites of phosphorylation. Activation and autophosphorylation. J. Biol. Chem. *277*, 42987–42996.

Halder, G., and Johnson, R.L. (2011). Hippo signaling: growth control and beyond. Development *138*, 9–22.

Hamaratoglu, F., Willecke, M., Kango-Singh, M., Nolo, R., Hyun, E., Tao, C., Jafar-Nejad, H., and Halder, G. (2006). The tumour-suppressor genes NF2/Merlin and Expanded act through Hippo signalling to regulate cell proliferation and apoptosis. Nat. Cell Biol. *8*, 27–36.

Hariharan, I.K., and Bilder, D. (2006). Regulation of imaginal disc growth by tumor-suppressor genes in *Drosophila*. Annu. Rev. Genet. *40*, 335–361.

Harvey, K., and Tapon, N. (2007). The Salvador-Warts-Hippo pathway - an emerging tumour-suppressor network. Nat. Rev. Cancer *7*, 182–191.

Jiao, S., Wang, H., Shi, Z., Dong, A., Zhang, W., Song, X., He, F., Wang, Y., Zhang, Z., Wang, W., et al. (2014). A peptide mimicking VGLL4 function acts as a YAP antagonist therapy against gastric cancer. Cancer Cell *25*, 166–180.

Jin, J., Arias, E.E., Chen, J., Harper, J.W., and Walter, J.C. (2006). A family of diverse Cul4-Ddb1-interacting proteins includes Cdt2, which is required for S phase destruction of the replication factor Cdt1. Mol. Cell *23*, 709–721.

King, R.W., Glotzer, M., and Kirschner, M.W. (1996). Mutagenic analysis of the destruction signal of mitotic cyclins and structural characterization of ubiquitinated intermediates. Mol. Biol. Cell *7*, 1343–1357.

Lallemand, D., Manent, J., Couvelard, A., Watilliaux, A., Siena, M., Chareyre, F., Lampin, A., Niwa-Kawakita, M., Kalamarides, M., and Giovannini, M. (2009). Merlin regulates transmembrane receptor accumulation and signaling at the plasma membrane in primary mouse Schwann cells and in human schwannomas. Oncogene *28*, 854–865.

Lee, J.-H., Kim, T.-S., Yang, T.-H., Koo, B.-K., Oh, S.-P., Lee, K.-P., Oh, H.-J., Lee, S.-H., Kong, Y.-Y., Kim, J.-M., and Lim, D.S. (2008). A crucial role of WW45 in developing epithelial tissues in the mouse. EMBO J. *27*, 1231–1242.

Lee, J.M., Lee, J.S., Kim, H., Kim, K., Park, H., Kim, J.Y., Lee, S.H., Kim, I.S., Kim, J., Lee, M., et al. (2012). EZH2 generates a methyl degron that is recognized by the DCAF1/DDB1/CUL4 E3 ubiquitin ligase complex. Mol. Cell *48*, 572–586.

Li, W., You, L., Cooper, J., Schiavon, G., Pepe-Caprio, A., Zhou, L., Ishii, R., Giovannini, M., Hanemann, C.O., Long, S.B., et al. (2010). Merlin/NF2 suppresses tumorigenesis by inhibiting the E3 ubiquitin ligase CRL4(DCAF1) in the nucleus. Cell *140*, 477–490.

Li, W., Cooper, J., Karajannis, M.A., and Giancotti, F.G. (2012). Merlin: a tumour suppressor with functions at the cell cortex and in the nucleus. EMBO Rep. *13*, 204–215.

Liu-Chittenden, Y., Huang, B., Shim, J.S., Chen, Q., Lee, S.J., Anders, R.A., Liu, J.O., and Pan, D. (2012). Genetic and pharmacological disruption of the TEAD-YAP complex suppresses the oncogenic activity of YAP. Genes Dev. *26*, 1300–1305.

Mani, T., Hennigan, R.F., Foster, L.A., Conrady, D.G., Herr, A.B., and Ip, W. (2011). FERM domain phosphoinositide binding targets merlin to the membrane and is essential for its growth-suppressive function. Mol. Cell. Biol. *31*, 1983–1996.

Overholtzer, M., Zhang, J., Smolen, G.A., Muir, B., Li, W., Sgroi, D.C., Deng, C.X., Brugge, J.S., and Haber, D.A. (2006). Transforming properties of YAP, a candidate oncogene on the chromosome 11q22 amplicon. Proc. Natl. Acad. Sci. USA *103*, 12405–12410.

Pan, D. (2010). The hippo signaling pathway in development and cancer. Dev. Cell *19*, 491–505.

Schulze, K.M., Hanemann, C.O., Müller, H.W., and Hanenberg, H. (2002). Transduction of wild-type merlin into human schwannoma cells decreases schwannoma cell growth and induces apoptosis. Hum. Mol. Genet. *11*, 69–76.

St John, M.A.R., Tao, W., Fei, X., Fukumoto, R., Carcangiu, M.L., Brownstein, D.G., Parlow, A.F., McGrath, J., and Xu, T. (1999). Mice deficient of Lats1 develop soft-tissue sarcomas, ovarian tumours and pituitary dysfunction. Nat. Genet. *21*, 182–186.

Tamori, Y., Bialucha, C.U., Tian, A.G., Kajita, M., Huang, Y.C., Norman, M., Harrison, N., Poulton, J., Ivanovitch, K., Disch, L., et al. (2010). Involvement of Lgl and Mahjong/VprBP in cell competition. PLoS Biol. *8*, e1000422.

Tapon, N., Harvey, K.F., Bell, D.W., Wahrer, D.C.R., Schiripo, T.A., Haber, D.A., and Hariharan, I.K. (2002). salvador Promotes both cell cycle exit and apoptosis in *Drosophila* and is mutated in human cancer cell lines. Cell *110*, 467–478.

Toji, S., Yabuta, N., Hosomi, T., Nishihara, S., Kobayashi, T., Suzuki, S., Tamai, K., and Nojima, H. (2004). The centrosomal protein Lats2 is a phosphorylation target of Aurora-A kinase. Genes Cells *9*, 383–397.

Xiao, L., Chen, Y., Ji, M., Volle, D.J., Lewis, R.E., Tsai, M.-Y., and Dong, J. (2011). KIBRA phosphorylation is regulated by the mitotic kinase aurora and protein phosphatase 1. J. Biol. Chem. *286*, 36304–36315.

Yang, X., Yu, K., Hao, Y., Li, D.M., Stewart, R., Insogna, K.L., and Xu, T. (2004). LATS1 tumour suppressor affects cytokinesis by inhibiting LIMK1. Nat. Cell Biol. *6*, 609–617.

Yi, C., Troutman, S., Fera, D., Stemmer-Rachamimov, A., Avila, J.L., Christian, N., Persson, N.L., Shimono, A., Speicher, D.W., Marmorstein, R., et al. (2011). A tight junction-associated Merlin-angiomotin complex mediates Merlin's regulation of mitogenic signaling and tumor suppressive functions. Cancer Cell *19*, 527–540.

Yin, F., Yu, J., Zheng, Y., Chen, Q., Zhang, N., and Pan, D. (2013). Spatial organization of Hippo signaling at the plasma membrane mediated by the tumor suppressor Merlin/NF2. Cell *154*, 1342–1355.

Yu, F.X., Zhao, B., Panupinthu, N., Jewell, J.L., Lian, I., Wang, L.H., Zhao, J., Yuan, H., Tumaneng, K., Li, H., et al. (2012). Regulation of the Hippo-YAP pathway by G-protein-coupled receptor signaling. Cell *150*, 780–791.

Zender, L., Spector, M.S., Xue, W., Flemming, P., Cordon-Cardo, C., Silke, J., Fan, S.T., Luk, J.M., Wigler, M., Hannon, G.J., et al. (2006). Identification and validation of oncogenes in liver cancer using an integrative oncogenomic approach. Cell *125*, 1253–1267.

Zhang, N., Bai, H., David, K.K., Dong, J., Zheng, Y., Cai, J., Giovannini, M., Liu, P., Anders, R.A., and Pan, D. (2010). The Merlin/NF2 tumor suppressor functions through the YAP oncoprotein to regulate tissue homeostasis in mammals. Dev. Cell *19*, 27–38.

Zhao, B., Wei, X., Li, W., Udan, R.S., Yang, Q., Kim, J., Xie, J., Ikenoue, T., Yu, J., Li, L., et al. (2007). Inactivation of YAP oncoprotein by the Hippo pathway is involved in cell contact inhibition and tissue growth control. Genes Dev. *21*, 2747–2761.

Zhao, B., Li, L., Lei, Q., and Guan, K.-L. (2010a). The Hippo-YAP pathway in organ size control and tumorigenesis: an updated version. Genes Dev. *24*, 862–874.

Zhao, B., Li, L., Tumaneng, K., Wang, C.Y., and Guan, K.L. (2010b). A coordinated phosphorylation by Lats and CK1 regulates YAP stability through SCF(β-TRCP). Genes Dev. *24*, 72–85.

Zhou, D., Conrad, C., Xia, F., Park, J.-S., Payer, B., Yin, Y., Lauwers, G.Y., Thasler, W., Lee, J.T., Avruch, J., and Bardeesy, N. (2009). Mst1 and Mst2 maintain hepatocyte quiescence and suppress hepatocellular carcinoma development through inactivation of the Yap1 oncogene. Cancer Cell *16*, 425–438.